LA-UR -85-1303

CONF-850247--3
RECEIVED BY OSTI MAY 06 1985

LA-UR--85-1303

DE85 010761

TITLE: Solar Wind-Magnetosphere Energy Input Functions

AUTHOR(S): L.F. Bargatze, R.L. McPherron and D.N. Baker

MASTER

SUBMITTED TO: Proceedings of the Chapman Conference on Solar-Wind Magnetosphere Energy Coupling, 12-15 February 1985, Pasadena, CA

Los Alamos Los Alamos National Laboratory
Los Alamos, New Mexico 87545

Solar-Wind Magnetosphere Energy Input Functions

L. F. Bargatze[1,2,3], R. L. McPherron[1,2], and D. N. Baker[3]

[1]Department of Earth and Space Sciences
University of California at Los Angeles
Los Angeles, CA 90024

[2]Institute of Geophysics and Planetary Physics
University of California at Los Angeles
Los Angeles, CA 90024

[3]University of California, Los Alamos National Laboratory
Los Alamos, NM 87545

IGPP Publication #2632
submitted to the
Proceedings of the Chapman Conference on
Solar Wind-Magnetosphere Energy Coupling

April 1985

ABSTRACT

A new formula for the solar wind-magnetosphere energy input parameter, P_i, is sought by applying the constraints imposed by dimensional analysis. Applying these constraints yields a general equation for P_i which is equal to $\rho V^3 \ell_{CF}^2 F(M_A,\theta)$ where, ρV^3 is the solar wind kinetic energy density and ℓ_{CF}^2 is the scale size of the magnetosphere's effective energy "collection" region. The function F which depends on M_A, the Alfvén Mach number, and on θ, the interplanetary magnetic field clock angle is included in the general equation for P_i in order to model the magnetohydrodynamic processes which are responsible for solar wind-magnetosphere energy transfer. By assuming the form of the function F, it is possible to further constrain the formula for P_i. This is accomplished by using solar wind data, geomagnetic activity indices, and simple statistical methods. It is found that P_i is proportional to $(\rho V^2)^{1/6} VBG(\theta)$ where, ρV^2 is the solar wind dynamic pressure and $VBG(\theta)$ is a rectified version of the solar wind motional electric field. Furthermore, it is found that $G(\theta)$, the gating function which modulates the energy input to the magnetosphere, is well represented by a "leaky" rectifier function such as $\sin^4(\theta/2)$. This function allows for enhanced energy input when the interplanetary magnetic field is oriented southward. This function also allows for some energy input when the interplanetary magnetic field is oriented northward.

Introduction

An important goal of solar-terrestrial physics is to understand how the rate of solar wind-magnetosphere energy transfer depends upon interplanetary and magnetospheric parameters. In the past, simple cross-correlation analyses have been used to establish the causal connection between enhanced geomagnetic activity and the variations of single solar wind parameters such as the solar wind plasma speed (V), the interplanetary magnetic field (IMF) strength (B), and the north-south orientation of the IMF vector (see review by Baker, 1985, in this volume, and references therein). Later, researchers began developing more complex formulas to correlate with geomagnetic indices. Such formulas include $\varepsilon = VB^2 \ell_o^2 \sin^4(\theta/2)$ (ℓ_o = 7 earth radii, θ is the IMF clock angle defined below), $V^2 B_s$, and VB_s ($B_s = -B_Z$ if $B_Z < 0.0$, $B_s = 0.0$ otherwise).

Here, we take a slightly different approach. Before cross-correlating any variables, we use the constraints imposed by dimensional analysis as a guide to develop a general formula for P_i, the rate of solar wind-magnetosphere energy transfer (Vasyliunas et al., 1982). This general equation is listed below:

$$P_i = \rho V^3 \ell_{CF}^2 F(M_A, \theta) \tag{1}$$

where, ρ is the solar wind plasma density, ℓ_{CF} is the Chapman-Ferraro scale length ($\ell_{CF} = (M_E^2/\mu_o \rho V^2)^{1/6}$), M_A is the Alfvén Mach number ($M_A^2 = (\mu_o \rho V^2/B_T^2)^{1/2}$), θ is the IMF clock angle, and F is a function whose dependence upon M_A and θ will be discussed below. Other quantities in these formulas include M_E, the earth's magnetic dipole moment, μ_o, the permeability of free space, B_T, the magnitude of the vector sum of the IMF

B_Y and B_Z components measured using geocentric solar magnetospheric (GSM) coordinates, and θ, the angle equal to the arc subtended by the GSM Z-axis and the $\vec{B}_T$

Equation 1 explicitly assumes that the amount of energy which is transferred from the solar wind to the magnetosphere is proportional to the amount of solar wind kinetic energy that is intercepted by an energy "collection" region on the magnetopause. Equation 1 includes the function F in order to model the magnetohydrodynamic interactions which are responsible for the energy transfer. Here, we assume as did Vasyliunas et al. (1982) that $F = M_A^{-2\alpha} G(\theta)$ where, α is the MHD coupling exponent, and $G(\theta)$ is a function which modulates the rate of energy input depending upon the orientation of the IMF.

Unfortunately, the energy input rate cannot be directly measured. It is customary instead to approximate P_i by using various indices of geomagnetic activity. In this study, we use the AL index to estimate P_i. This index is sensitive to the amount of current which flows in the westward electrojet (Baumjohann, 1985, this volume). The AL index, however, does not respond instantaneously to the rate of solar wind energy input. Hence, one must account for the time delay between solar wind energy input and the enhancement of current flow in the westward electrojet. We do this by convolving an average AL index impulse response filter, f, with the solar wind input time series (see papers by Bargatze et al., 1985; McPherron et al., 1985; and Clauer, 1985; all this volume). In this light, Equation 1 becomes:

$$P = f * (\rho V^3 \, \ell_{CF}^2 \, M_A^{-2\alpha} \, kG(\theta)) \tag{2}$$

where the star represents convolution and the normalization constant k has been introduced such that G(θ) is now defined to vary between 0.0 and 1.0. In going from Equation 1 to Equation 2, the i-subscript has been dropped from P_i; this is done to emphasize the fact that the AL index, a geomagnetic activity index, has been used to estimate P_i, the solar wind energy input parameter.

In the remainder of this study, three different methods are employed to investigate the dependence of P_i upon solar wind variables. Each of these methods is based on a simple statistical technique and on a modified version of Equation 2. The analyses were completed using a data base that includes IMP-8 solar wind data from 1973-4, ISEE-3 solar wind data from 1978, and the corresponding values of the AL index. The results are presented in three separate sections below.

REGRESSION ANALYSIS RESULTS

The formula which provides the basis for the regression analysis is easily obtained from Equation 2 after substituting for the Chapman-Ferraro scale length:

$$\log\left(\frac{P}{\mu_o^{-1/3} M_E^{2/3} \rho^{2/3} V^{7/3}}\right) = \alpha \log(M_A^{-2}) + \log(kf*G(\theta)) \tag{3}$$

Equation 3 is that for a straight line, $Y = \alpha X + B$, where, X and Y are logarithmic variables, α is the line's slope, and log(kf*G(θ)) is the line's Y-axis intercept. Strictly speaking, Equation 3 is a valid representation of Equation 2 if and only if the quantities $\rho V^3 \ell_{CF}^2$ and M_A^2

are approximately constant since these terms have been removed from the convolution with the impulse response function, f.

To use Equation 3, the data set was separated into twelve bins depending on the value of $G^{-1}(f*G(\theta))$ where, $G(\theta)$ is assumed to be equal to $\sin^4(\theta/2)$ and G^{-1} is its trigonometric inverse function. Each bin corresponds to a 15° range in θ starting with $0^{\circ} < \theta < 15^{\circ}$ (a nearly northward IMF) and ending with $165^{\circ} < \theta < 180^{\circ}$ (a nearly southward IMF). The data within each bin were used s input to a simple linear regression analysis routine in order to estimate the slope and intercept of the best fit line through the distribution.

Figure 1 is a scatter plot of the logarithmic variables which was made by assuming that P is equal to the AL index multiplied by an energy conversion factor of 3×10^8 ((J/s)/nT) (Perreault and Akasofu, 1978). For this figure, the value of θ was restricted to lie between 135° and 150°. The best fit line has a slope equal to 0.54; the linear correlation coefficient is equal to 0.66. Figure 2 is a summary of all of the α-slope estimates plotted as a function of θ. The error in the α-estimates are shown using 2-σ error bars. For northward IMF, almost all of the slope estimates lie between 0.0 and 0.4; however, all of the corresponding regression coefficients are smaller than 0.3. For southward IMF, all but one of the slope estimates lie between 0.4 and 0.6. The regression coefficients are higher reaching values near 0.7.

HISTOGRAM ANALYSIS RESULTS

For this section only, we define a new MHD coupling exponent, α', which is equal to $1.0 - \alpha$. We do this in order to directly compare the results of this section with the results of a histogram analysis performed by Kan and Akasofu (1982). Given that $\alpha' = 1.0 - \alpha$, one can readily manipulate Equation 2 to yield:

$$P = f*(\frac{1}{\mu_o} VB_T^2 \, k\ell_{CF}^2 \, M_A^{2\alpha'} \, G(\theta)) \tag{4}$$

The histogram analysis equation is obtained directly from Equation 4 by solving for α' explicitly:

$$\alpha' = \log[P/(f*(\frac{1}{\mu_o} VB_T^2 \, k\ell_{CF}^2 \, G(\theta)))]/\log(M_A^2) \tag{5}$$

To perform the analysis, it is assumed once again that P is proportional to the AL index and that $G(\theta)$ is equal to $\sin^4(\theta/2)$. Then, each set of data points is used as input to Equation 5 to obtain an estimate of α'. The "best" estimate of α' is determined by histogramming all of the α'-estimates to find the most frequently occurring α'-value.

Figure 3 shows the result of the AL histogram analysis. Note that the distribution peaks between 0.5 and 0.55 and that the half-width of the distribution which provides an estimate of error is about 0.1. This result is in accord with the regression analysis results which suggest that α is equal to 0.5 (since $\alpha = 1.0 - \alpha'$).

GATING FUNCTION ANALYSIS

Rearranging Equation 2, one obtains the formula used to calculate the empirical dependence of $G(\theta)$ upon θ:

$$G(\theta) = \frac{P}{f*(\rho V^3 k \ell_{CF}^2 M_A^{-1})} \tag{6}$$

Note that α was assumed to be equal to 0.5 to yield this equation. Before analysis, the data were separated into twelve bins depending on the average value of θ. Each data bin corresponds to a 15° range in θ The binned data sets were then used as input to Equation 6 in order to find the aver of $G(\theta)$ within each bin. Since the $G(\theta)$ term has been removed from the convolution with f, we have limited the analysis to include only those intervals during which θ was approximately constant.

The results are displayed in Figure 4. Also plotted are two solid lines which show the variation $\sin^4(\theta/2)$ and $U(\theta)\cos(\theta)$ versus θ ($U(\theta) = 0.0$ if $\theta < 90^\circ$ and $U(\theta) = -1.0$ if $\theta > 90^\circ$). These are the gating functions used in the definitions of ε and VB_s respectively. In Figure 4a, the $G(\theta)$-estimates have been normalized such that they approach 1.0 at $\theta = 180^\circ$. Note that the $G(\theta)$-estimates do not approach zero asymptotically as θ approaches 0°. This is likely due to the errors involved in the analysis or perhaps due to the effects of energy input to the magnetosphere via viscous processes (Axford, 1964). This "error" baseline corresponds to an AL index value of about -50 nT. Figure 4b shows the $G(\theta)$-estimates renormalized after the "error" baseline has been subtracted out. These estimates agree quite well with the $\sin^4(\theta/2)$ curve.

CONCLUSION

In summary, we have used the constraints imposed by dimensional analysis and three different statistical techniques to examine the relationship governing energy transfer from the solar wind to the magnetosphere. Two of these techniques, the regression technique and the histogram technique, have been used to find whether P_i is better represented by a parameter such as ε which is related to flow of energy described by the Poynting vector of the solar wind or by a parameter such as VB_s which is related to the solar wind motional electric field. Both the regression analysis results and the histogram analysis results suggest that the MHD coupling exponent, α, is equal to 0.5 ± 0.1. If α is equal to 0.5, the rate of energy transfer is given by $\rho V^3 k \ell_{CF}^2 M_A^{-1} G(\theta)$. This function is proportional to $(\rho V^2)^{1/6} VBG(\theta)$ where, ρV^2 is the solar wind dynamic pressure and $VBG(\theta)$ is a rectified version of the solar wind motional electric field. Thus, the results suggest that P_i is more closely related to the strength of the solar wind motional electric field. Since P_i depends upon the solar wind dynamic pressure, the scale length of the magnetosphere which is inversely proportional to ρV^2 also plays an important role in determining the rate of energy transfer.

The above conclusions differ from the conclusions reached by Kan and Akasofu (1982) who found that $P_i = \varepsilon$. Their conclusion is based on a histogram analysis similar to the one presented here except that they modeled P_i using U_T, a measure of the total rate of magnetospheric energy dissipation (Perreault and Akasofu, 1978). However, it appears that they have not performed a completely general analysis. In particular, they have implicitly chosen a value for the constant k which is about an order of magnitude larger than the value of k that we have found using the regression technique and the 1978 data base which includes U_T (the U_T results are not presented here due to lack of space; they are in general agreement with the AL index results). Referring back to Equation 3, one finds that the constant k determines the Y-axis intercept of the line which best relates the two logarithmic variables. Hence, one cannot freely assume any value for k in order to perform a histogram analysis; it is crucial to use a value of k which is consistent with the results of regression analysis.

The results of the gating function analysis suggest that $G(\theta)$ is best represented by a "leaky" rectifier function such as $\sin^4(\theta/2)$ which is used in the definition of ε. We use the term leaky since a function like $\sin^4(\theta/2)$ allows for a small amount of energy input when the IMF is northward. In contrast, the half-wave rectifier function like that used in the definition of VB_s does not allow for any energy input when the IMF is northward. Both, of course, allow for enhanced energy input when the IMF is oriented southward.

The highest correlation coefficients of the analyses presented here lie near 0.7. If the correlation coefficients were much lower, one might question the validity of the theoretical guidelines provided by dimensional analysis which were used to obtain the original, general formula for P_i. Still, the magnitude of the correlation coefficients suggests that the model that we have used here could be improved. In fact, Vasyliunas et al. (1982) have suggested using a more complete model that incorporates magnetosphere-ionosphere coupling. Unfortunately, we cannot test this model until a high-time resolution data base which includes the ionospheric Pedersen conductivity becomes available.

Acknowledgements. The IMP-8 magnetometer data were supplied by researchers at the Goddard Space Flight Center and the ISEE-3 magnetometer data were supplied by researchers at the Jet Propulsion Laboratory. The AE indices were provided by the World Data Center, Boulder, Colorado. This work was supported at Los Alamos by the Institute of Geophysics and

Planetary Physics and was done under the auspices of the United States Department of Energy. This work was supported at the University of California at Los Angeles by the National Science Foundation, grant ATM 83-18200, by the Office of Naval Research, grant N00014-84-C-0158, and by the National Aeronautics and Space Administration, grant NGL-05-007-004.

REFERENCES

Axford, W. I., Viscous interaction between the solar wind and the earth's magnetosphere, _Planet. Space Sci._, _12_, 45, 1964.

Baker, D. N., Statistical Analyses in the study of solar wind-magnetosphere coupling, in _Solar Wind-Magnetosphere Coupling_, edited by Y. Kamide and J. A. Slavin, (submitted), Pasadena, 1985.

Bargatze, L. F., D. N. Baker, and R. L. McPherron, Magnetospheric response to solar wind variations, in _Solar Wind-Magnetosphere Coupling_, edited by Y. Kamide and J. A. Slavin, (submitted), Pasadena, 1985.

Baumjohann, W., Merits and limitations of the use of geomagnetic indices in solar wind-magnetosphere coupling, in _Solar Wind-Magnetosphere Coupling_, edited by Y. Kamide and J. A. Slavin, (submitted), Pasadena, 1985.

Clauer, C. R., The technique of linear prediction filters applied to studies of solar wind-magnetosphere coupling, in _Solar Wind-Magnetosphere Coupling_, edited by Y. Kamide and J. A. Slavin, (submitted), Pasadena, 1985.

Kan, J. R., and S.-I. Akasofu, Dynamo process governing solar wind-magnetosphere energy coupling, _Planet. Space Sci._, _30_, 367, 1982.

McPherron, R. L., D. N. Baker, and L. F. Bargatze, Linear filters as a method of real-time prediction of geomagnetic activity, in _Solar Wind-Magnetosphere Coupling_, edited by Y. Kamide and J. A. Slavin, (submitted), Pasadena, 1985.

Perreault, P. and S.-I. Akasofu, A study of geomagnetic storms, _J. Roy. Astron. Soc._, _54_, 547, 1978.

Vasyliunas, V. M., J. R. Kan, G. L. Siscoe, and S.-I. Akasofu, Scaling relations governing magnetospheric energy transfer, Planet. Space Sci., 30, 359, 1982.

FIGURE CAPTIONS

Figure 1. The scatter plot of the logarithmic variables, $P/\rho V^3 \ell_{CF}^2$ and M_A^{-2}, for θ between 135^o and 150^o is shown. The slope of the regression line, α, is equal to 0.54; the regression coefficient, R, is equal to 0.66. The constant k_1 used in defining the ordinate is equal to $\mu_o^{-1/3} M_E^{2/3}$; k_1 should not be confused to the constant k referred to in the text.

Figure 2. Summary of the α regression results. Values of α are plotted versus the IMF clock angle, θ. 2-σ error bars are plotted for each data point.

Figure 3. The number of occurrences of α' is plotted versus the magnitude of α'. Note that α' is equal to $1.0 - \alpha$.

Figure 4. Empirical estimates of the gating function, $G(\theta)$, are plotted versus the IMF clock angle, θ. Two functions, $\sin^4(\theta/2)$ (upper solid curve) and $U(\theta)\cos(\theta)$ (lower solid curve), are shown for comparison. In Figure 4a, the empirical $G(\theta)$-values were normalized such that they approach 1.0 for $\theta = 180^o$. In Figure 4b, an "error" baseline was subtracted before normalizing the $G(\theta)$-values.

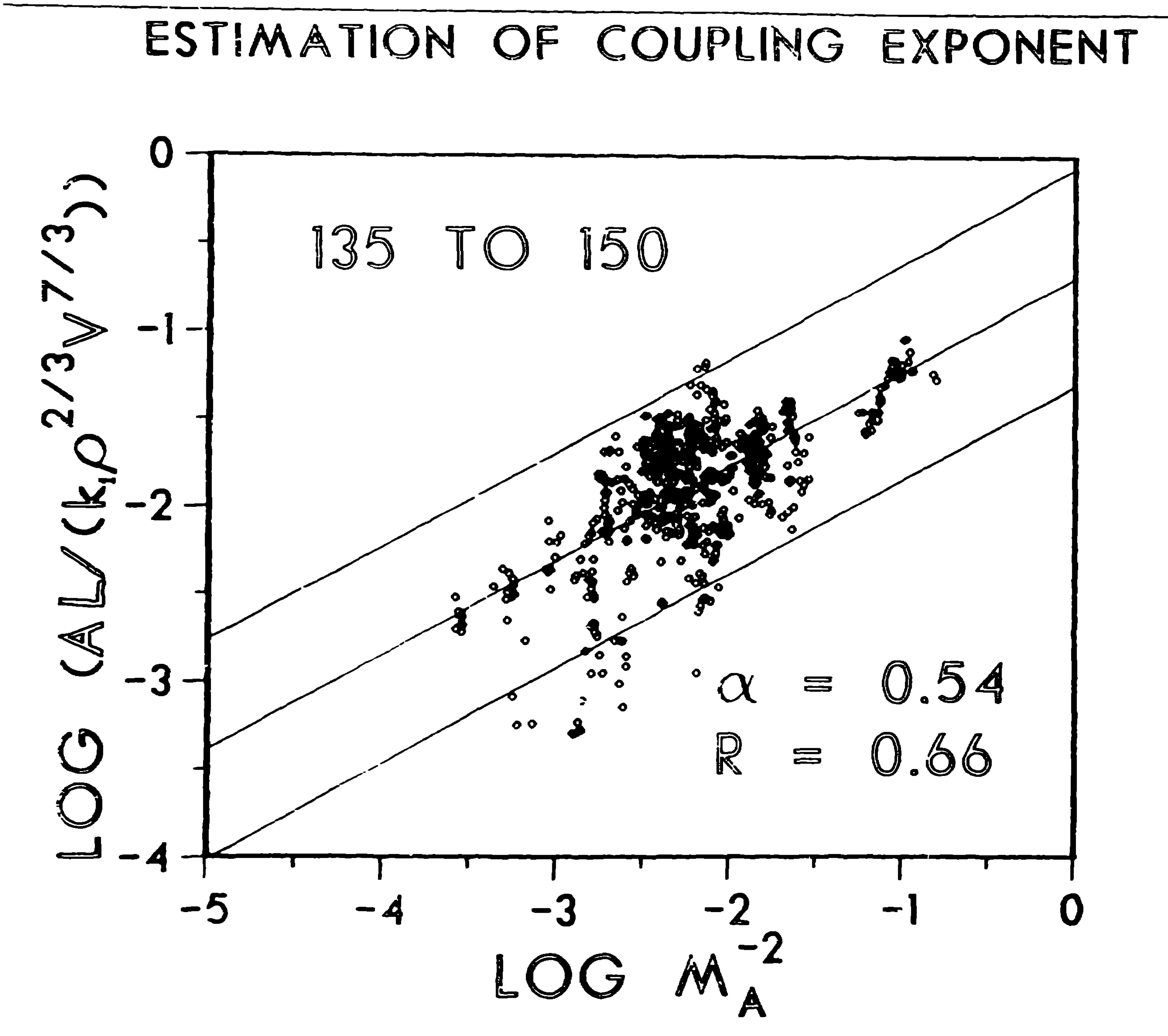
ESTIMATION OF COUPLING EXPONENT
135 TO 150
$\alpha = 0.54$
$R = 0.66$
$\mathrm{LOG}\,(AL/(k_1\rho^{2/3}V^{7/3}))$
$\mathrm{LOG}\,M_A^{-2}$
0
-1
-2
-3
-4
-5
-4
-3
-2
-1
0

FIGURE 1.

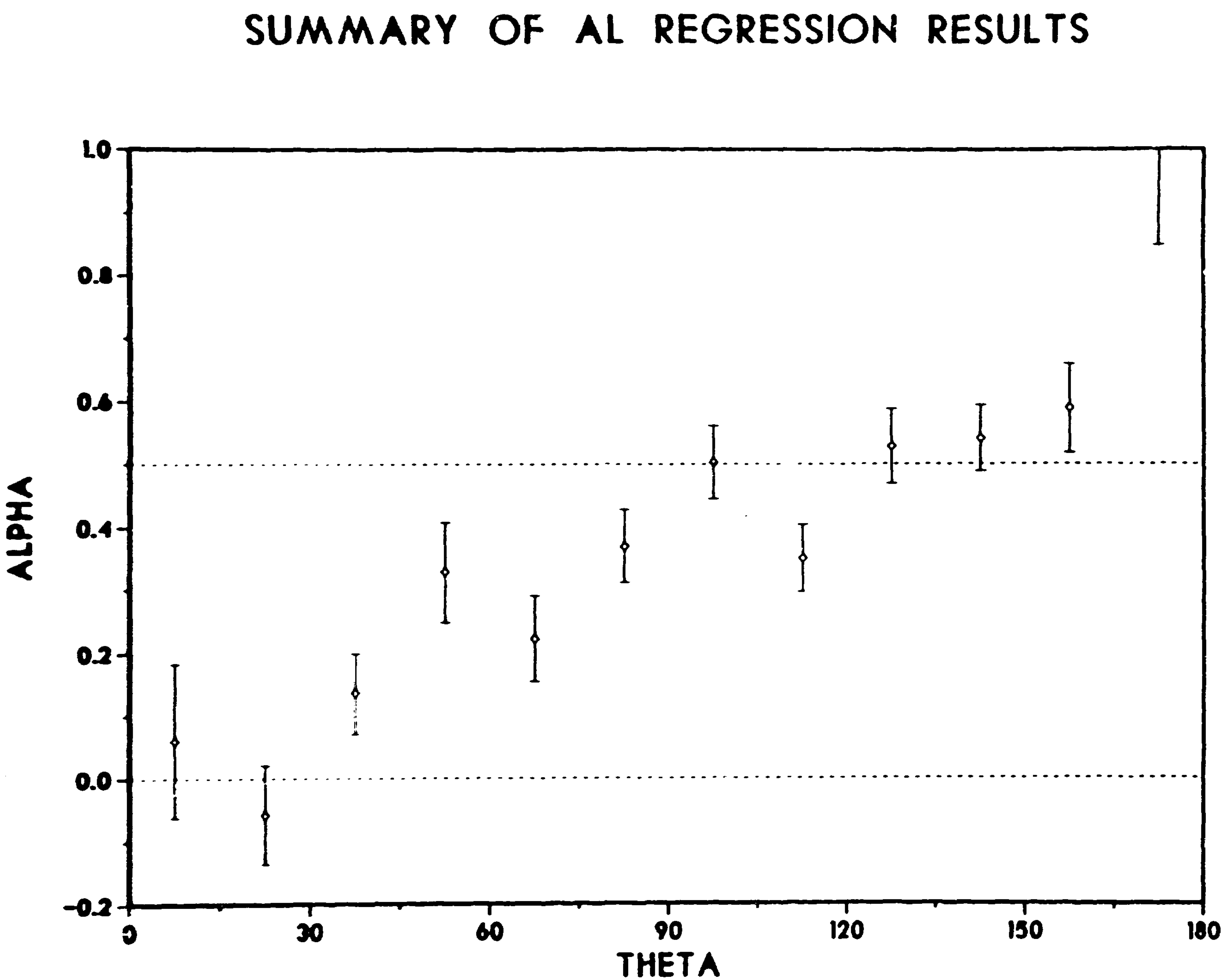
SUMMARY OF AL REGRESSION RESULTS
ALPHA
1.0
0.8
0.6
0.4
0.2
0.0
-0.2
0
30
60
90
120
150
180
THETA

FIGURE 2.

ALPHA' OCCURRENCE HISTOGRAM -- AL INDEX

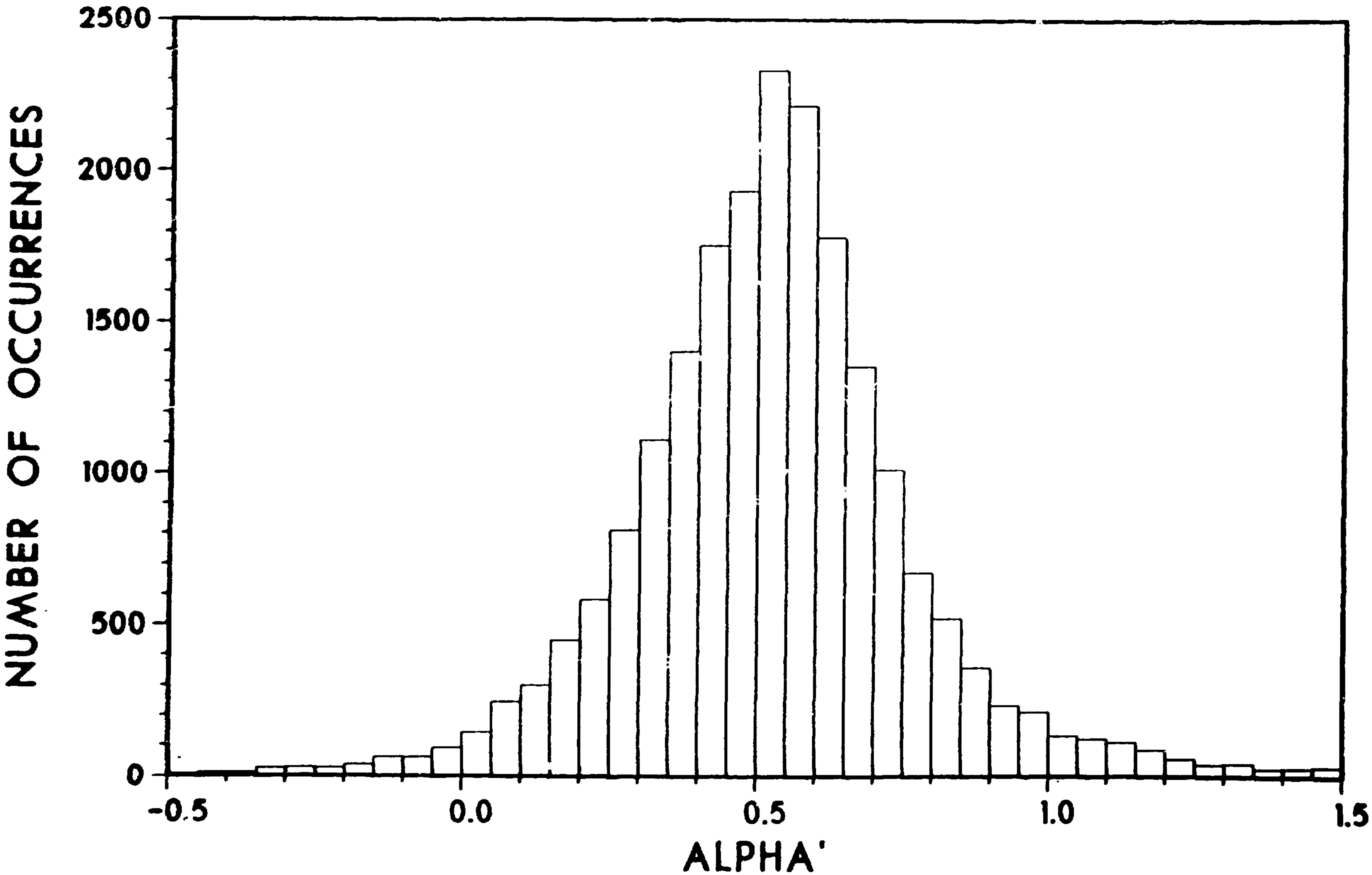

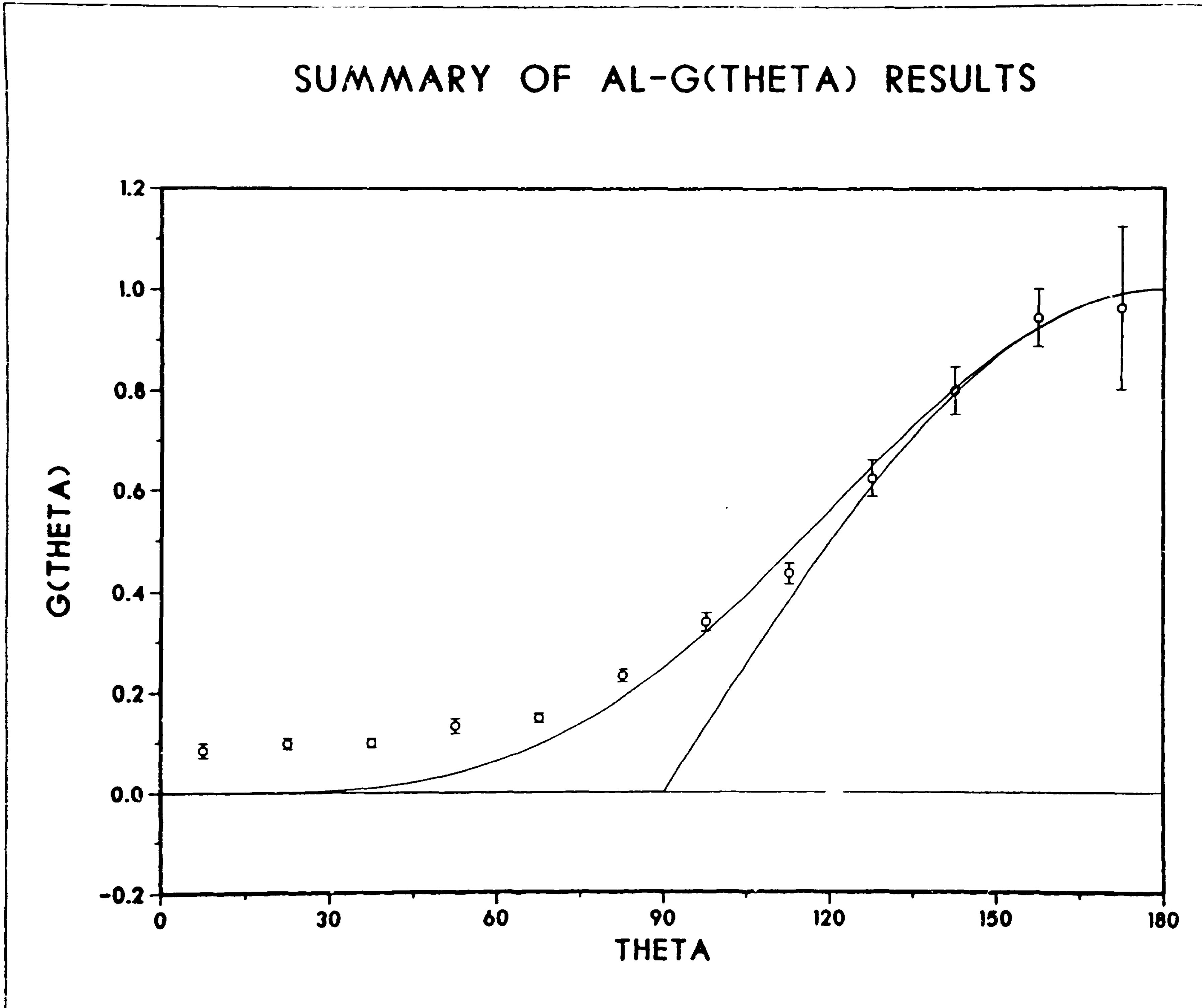
SUMMARY OF AL-G(THETA) RESULTS
G(THETA)
1.2
1.0
0.8
0.6
0.4
0.2
0.0
-0.2
0
30
60
90
120
150
180
THETA

FIGURE 4A.

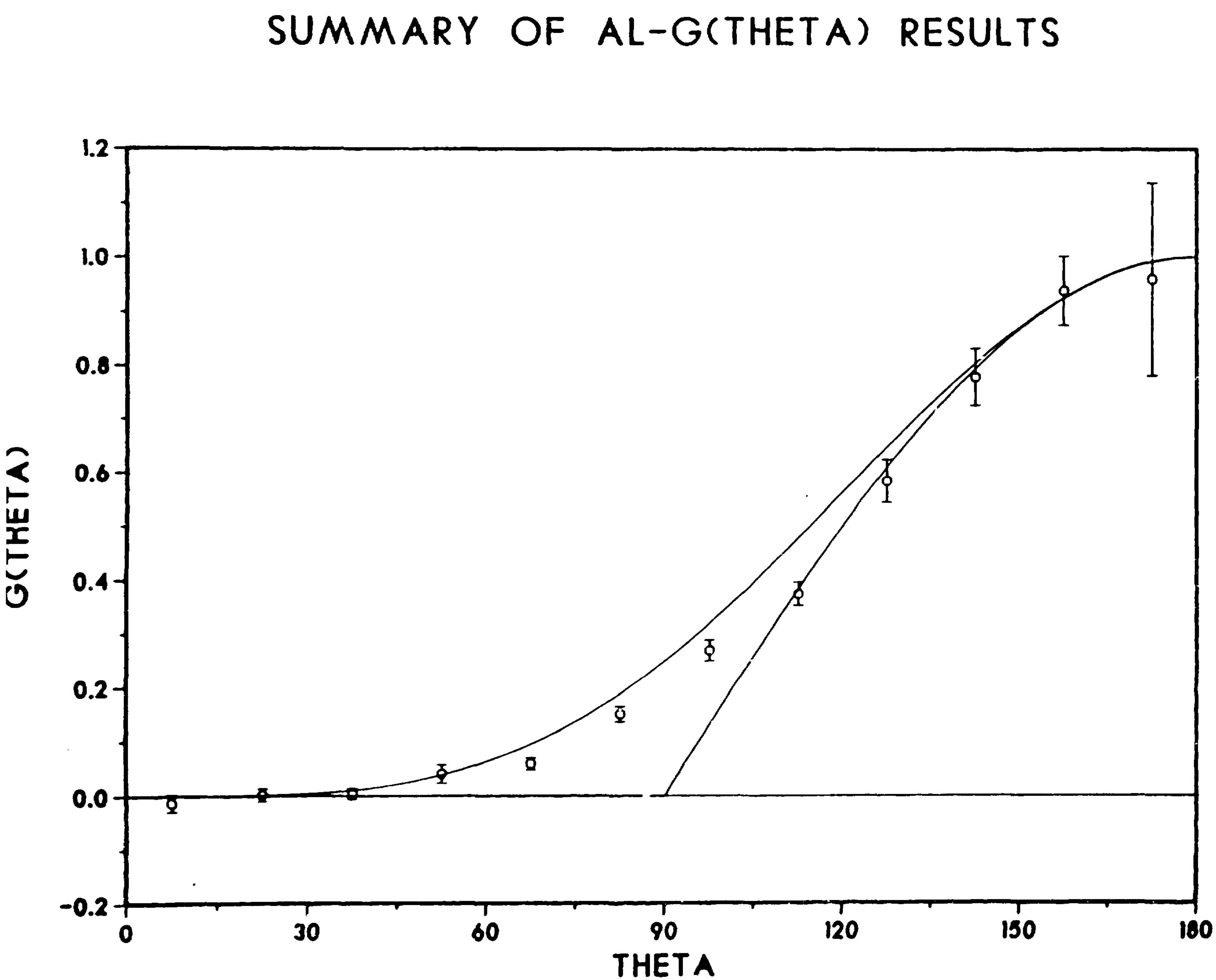
SUMMARY OF AL-G(THETA) RESULTS
G(THETA)
THETA
1.2
1.0
0.8
0.6
0.4
0.2
0.0
-0.2
0
30
60
90
120
150
180

FIGURE 4B.